Friction and energy dissipation at the atomic scale: A review

I. L. Singer[a)]
Code 6170, U.S. Naval Research Laboratory, Washington, DC 20375

(Received 28 January 1994; accepted 12 May 1994)

Discussions of energy dissipation during friction processes have captured the attention of engineers and scientists for over 300 years. Why then do we know so little about either dissipation or friction processes? A simple answer is that we cannot see what is taking place at the interface during sliding. Recently, however, devices such as the atomic force microscope have been used to perform friction measurements, characterize contact conditions, and even describe the ''worn surface.'' Following these and other experimental developments, friction modeling at the atomic level—particularly molecular dynamics (MD) simulations—has brought scientists a step closer to ''seeing'' what takes place during sliding contact. With these investigations have come some answers and new questions about the modes and mechanisms of energy dissipation at the sliding interface. This article will review recent theoretical and experimental studies of friction processes at the atomic scale. Theoretical treatments range from simple, analytical models of two-dimensional, coupled ball-spring systems at 0 K, to more complex MD simulations of three-dimensional arrays of hydrogen- and hydrocarbon-terminated surfaces at finite temperatures. Results are presented for the simplest yet most practical cases of sliding contact: sliding without wear. Sliding without friction is seen in weakly interacting systems. Simple models can easily explain the energetics of such friction processes, but MD studies are needed to explore the dynamics (excitation modes, energy pathways,...) of thermally excited atoms interacting in three-dimensional fields. These studies provide the first atomic-scale models for anisotropic friction and boundary lubrication. Friction forces at atomic interfaces must ultimately be measured at the macroscopic level; these measurements, which depend on the mechanical properties of the measuring system, are discussed. Two rather unique experimental studies of friction are also reviewed. The first employs a ''surface force apparatus'' to measure adhesion and friction between surfactant monolayers. The correlation of adhesion *hysteresis* and friction provides a new mechanism of friction; moreover, the interpretation for the effect—hysteresis from entanglement of the molecular chains during a phase transformation—implies that the dynamics are taking place at an accessible time scale (seconds to minutes). The second study extends the time domain at which friction can be measured to the nanosecond scale. A quartz-crystal oscillator is used to monitor the viscosity of monolayer liquids and solids against solid surfaces. Interfaces slip angstroms in nanoseconds. Modelers have suggested a variety of mechanisms for this atomic-scale friction process, from defect-mediated sliding to electron drag effects. The article ends by identifying the vast, barely charted time-space domain (micro-to-pico time and length scales) in which experiments are needed to further understand the dynamic aspects of friction processes.

I. BACKGROUND

Friction can now be studied at the atomic scale, thanks to developments in the past decade of a variety of experimental techniques.[1] The most well known, often referred to as proximal probes, have evolved from scanning tunneling microscopy (STM);[2] they include atomic force microscopy (AFM)[3] and its sliding companion friction force microscopy, (FFM).[4–6] These probes allow friction to be studied with atomic resolution in all three dimensions. Another proximal probe, generically known as a surface force apparatus (SFA), affords atomic resolution only in the vertical direction, but allows direct measurement and/or control of micrometer-sized areas of contact in the lateral direction.[7–14] A very recent technique, based on the quartz crystal microbalance (QCM), permits sliding friction processes to be studied at the angstrom level and at time scales in the nanosecond range.[15–17]

Although friction processes may originate at the sliding interface, the measurement of friction is usually performed by macroscopic devices—springs, levers, dashpots, etc.—often located far from the interface. In order to link measured frictional forces with theory, it has been necessary to examine the influence of mechanical parameters, such as stiffness, on friction measurements, not an unfamiliar problem to tribologists.[18,19] Proximal probes, however, are sensitive to mechanical properties of the probe as close as the first atomic layer of the tip and as far away as the compliant lever arm.[4,20–22]

[a)]E-mail: singer@chem.nrl.navy.mil

Report Documentation Page

Form Approved
OMB No. 0704-0188

1. REPORT DATE	2. REPORT TYPE	3. DATES COVERED
1994		**00-00-1994 to 00-00-1994**

4. TITLE AND SUBTITLE	5a. CONTRACT NUMBER
Friction and energy dissipation at the atomic scale: A review	5b. GRANT NUMBER
	5c. PROGRAM ELEMENT NUMBER
6. AUTHOR(S)	5d. PROJECT NUMBER
	5e. TASK NUMBER
	5f. WORK UNIT NUMBER
7. PERFORMING ORGANIZATION NAME(S) AND ADDRESS(ES) **Naval Research Laboratory,Code 6170,4555 Overlook Avenue, SW,Washington,DC,20375**	8. PERFORMING ORGANIZATION REPORT NUMBER
9. SPONSORING/MONITORING AGENCY NAME(S) AND ADDRESS(ES)	10. SPONSOR/MONITOR'S ACRONYM(S)
	11. SPONSOR/MONITOR'S REPORT NUMBER(S)

12. DISTRIBUTION/AVAILABILITY STATEMENT
Approved for public release; distribution unlimited

13. SUPPLEMENTARY NOTES

14. ABSTRACT

15. SUBJECT TERMS

16. SECURITY CLASSIFICATION OF:			17. LIMITATION OF ABSTRACT	18. NUMBER OF PAGES	19a. NAME OF RESPONSIBLE PERSON
a. REPORT **unclassified**	b. ABSTRACT **unclassified**	c. THIS PAGE **unclassified**		**12**	

The opening of experimental studies of friction at the nanometer and nanosecond scale has attracted theorists equipped to model physical and chemical processes at these scales. Surface scientists are now using sophisticated solid-state potentials to calculate mechanical interactions between surfaces.[22] Friction force calculations are performed either analytically or by molecular dynamics (MD) simulations.[23,24] MD simulation affords the added opportunity of using video animation to study friction processes. For the first time, scientists can ''see what is happening'' at the otherwise buried sliding interface. As you will read shortly, they see atomic and molecular excitation modes (vibrations, bending, and rotations), electron–hole excitations, density waves, and molecular interdigitation, to name a few. Once the modes are identified, physicists and chemists can address perhaps the most fundamental but least understood aspect of friction: energy dissipation processes. While it has been known for centuries[25,26] that most frictional energy dissipates as heat, neither the macroscopic nor microscopic mechanisms of energy dissipation have been fully explained. Adhesion and deformation contributions to energy dissipation in friction have recently been discussed by Johnson.[27] Here I review some recent theoretical and experimental studies of atomic-scale friction behavior and modes of energy dissipation.

Before launching into the studies, it is useful to review the thermodynamic criteria used to study energy dissipation. Clearly, if friction processes generate heat, they are irreversible and cannot be treated by classical thermodynamics. If, however, each step in a sliding interaction is executed with infinite slowness and with the two couples always in equilibrium (never an unbalanced force), then the process may be considered reversible. In such a quasistatic process, sliding can be achieved with zero friction. Real systems can *approximate* such reversible, adiabatic processes so long as the rate at which each step is taken is much slower than the relaxation time of the system.[28] However, any instability in the mechanical system that leaves unbalanced forces will result in an irreversible process in which energy is lost (or, more precisely, unrecoverable). In a mechanical system, where force F acts over a distance r, the energy lost over a cycle is given by

$$\Delta U = \oint F\, dr. \tag{1}$$

In an atomic sliding calculation, a cycle can be a translation across some periodic distance of the lattice, e.g., one atomic spacing. In an experiment, one cycle can be a single pass over a surface, including the making and breaking of the contact.

This article is presented in the following sequence. The second section deals with theoretical approaches used to examine friction processes and friction measurements at the atomic scale. Conditions that can give zero friction and finite friction in simple systems are presented. Two molecular dynamics simulations of more realistic yet ''wearless'' friction studies are described and modes of energy dissipation are identified. The third section presents two experimental approaches that have succeeded in identifying microscopic friction process; in both cases, energy losses are identified with hysteresis losses in the system. The fourth section summarizes our understanding of interfacial friction processes and energy dissipation mechanisms, and the fifth section considers ways that atomistic approaches can be used to solve practical problems in tribology.

II. THEORETICAL APPROACHES

A. Frictionless sliding

Two analytical studies that identify conditions for zero friction and the transition to finite friction are reviewed. The first investigates the potential seen by a moving atom, while the second examines the force experienced by the tip of a FFM. Although both present surface interactions at 0 K, they establish base line criteria for zero friction systems and measurements of zero friction by which more general calculations can be evaluated.

McClelland[29,30] describes the sliding friction behavior of a simple two-dimensional couple consisting of two substrates: the stationary upper substrate has an atom B_0 attached to a spring while the moving lower substrate consists of equally spaced, rigid atoms (see Fig. 1). Because of the periodicity of the lower layer, the entire sliding behavior can be analyzed by following the motion of atom B_0 across one atomic spacing. According to this independent oscillator (IO) model, atom B_0 experiences forces exerted by a spring above and the atoms below; the forces are derived from potentials V_{BB} and V_{AB}, respectively. As the lower substrate moves, the combined interaction potential V_S changes. The changing potential and the atomic trajectory of atom B_0 are depicted in the five sketches running left to right across the figure. The upper sketches represent a ''strong'' interaction and the lower, a ''weak'' interaction. The atom's position on a spring is shown as an open circle and its position in the potential V_S by a solid circle. In a ''strong'' potential, the atom is initially repelled to the right; then beyond half an atomic spacing, it ''snaps'' back to the left, the atomic equivalent of ''stick-slip.'' The snap back, or ''plucking'' motion, can be understood in terms of the evolving shape of potential V_S. In an adiabatic process, an atom must always sit at a minimum in the potential well. As can be seen, however, the position of the atom at (d) is only a local minimum, which disappears by position (e). At the moment the local metastable minimum ''flattens out,'' there are unbalanced forces on atom B_0; to regain an equilibrium state, the atom falls to the position of the stable minimum. Since this transition does not occur under equilibrium conditions, the process is irreversible and the energy lost in the fall cannot be reused to assist the sliding process. Stated in more physical terms, the strain energy put into stretching the spring at B_0 is not recovered locally; instead, it is converted into vibrational motion which dissipates into the substrate (as heat).

This instability can be avoided by using a ''weaker'' interaction potential. As shown in the lower sequence of sketches in Fig. 1, the weaker potential *does not develop a local minimum*. The atom moves smoothly through a repulsive then an attractive force field, first being repelled by, then pushing, the lower substrate. Since the system remains in equilibrium throughout the cycle, no energy is dissipated and

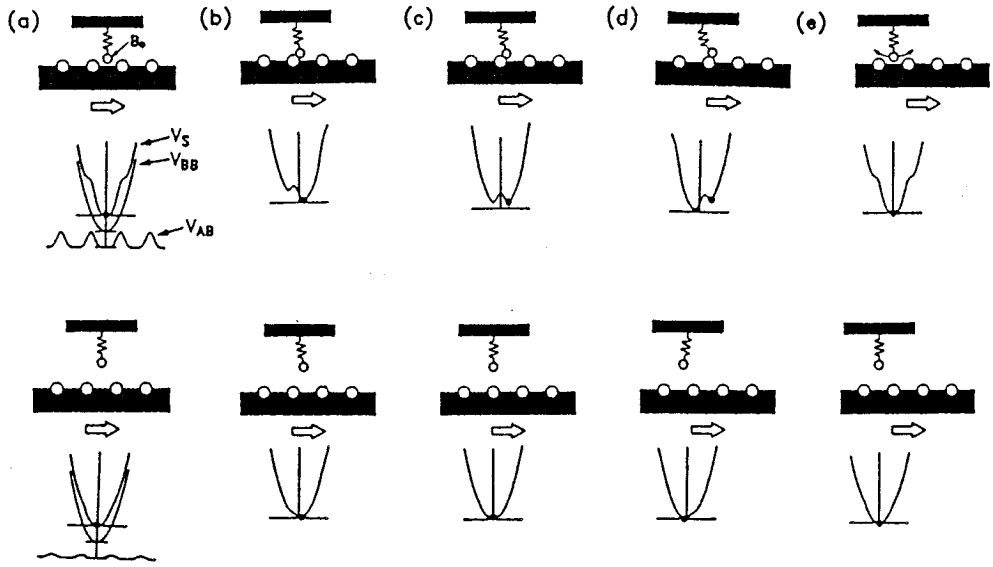

FIG. 1. Two representations of the motion of atom B_0 in the independent oscillator model: atom-on-spring and atom-in-potential. Top and bottom rows depict strong and weak interfacial interactions, respectively. The left-most diagrams display the relevant potentials (see text); subsequent panels illustrate the response of B_0 to progressive sliding of the lower layer of atoms. The location of atom B_0 is represented by a black dot in the combined potential V_S plotted below each atom-on-spring diagram (Refs. 29 and 30).

the friction force is zero. McClelland then gives more precise criteria for stability and shows that qualitatively similar friction behavior occurs with other more complex sliding couples.

Tomanek *et al.*[31–33] also describe conditions associated with frictionless sliding, emphasizing the mechanical proper ties of the apparatus as well as the strength and shape of the interatomic potentials. They present two idealized models for a FFM tip interacting with an atomic surface, only one of which is presented here. Called a ''realistic-friction microscope'' by the authors, the model accounts for the elasticity of the FFM as well as the external load F_{ext} and the surface interaction potential.

Figure 2 shows a FFM, with a horizontal spring that pulls the spring-tip assembly along the interface potential of the substrate. The tip experiences the combined force of the interface potential and F_{ext}. As the tip moves across the sur-

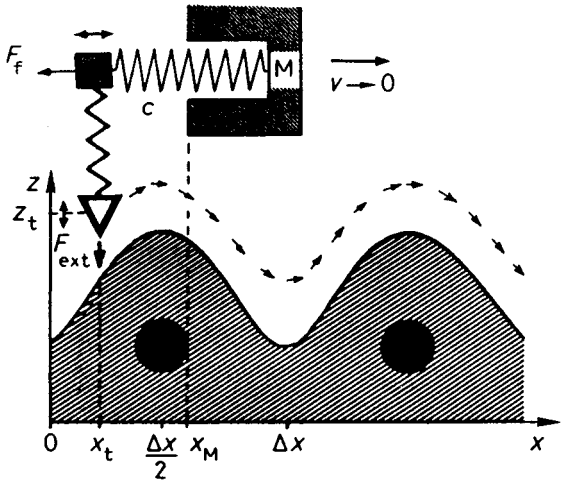

FIG. 2. Model of a FFM. External suspension M is guided along a horizontal surface in the x direction. The load F_{ext} is kept constant along the trajectory shown by arrows. The spring-tip assembly is elastically coupled to the suspension M in the horizontal direction by a spring of constant c. The friction force F_f is related to the elongation $x_t - x_M$ of the horizontal spring from its equilibrium value (Refs. 31 and 32).

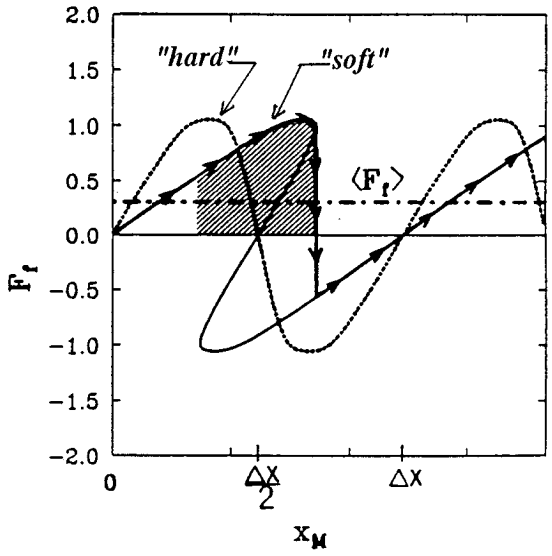

FIG. 3. The friction force F_f as a function of the FFM position x_M for a hard and soft spring and the average friction force $\langle F_f \rangle$ for a soft spring (Refs. 31 and 32).

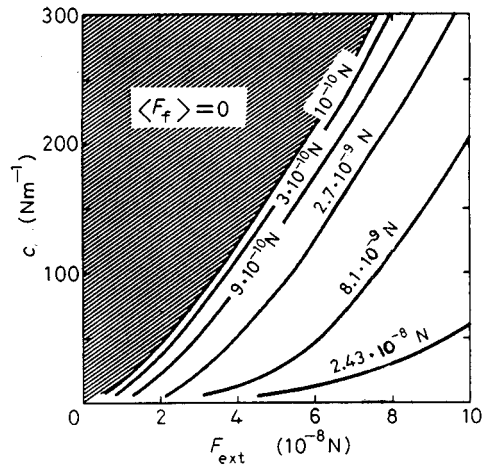

FIG. 4. Contour plot of the average friction force $\langle F_f \rangle$ per atom as a function of the load F_{ext} and the horizontal spring constant c (for monoatomic Pd tip on graphite) (Refs. 31 and 32).

face, the horizontal spring elongates by an amount, $x_M - x_t$, which depends on the stiffness c of the horizontal spring. For a "hard" spring ($c > c_{\text{crit}}$), both the tip trajectory and the F_f curve are single-valued functions of x_M; an example of the latter curve is labeled "hard" in Fig. 3. Since the positive and negative excursions of F_f are the same over a cycle, the average friction force $\langle F_f \rangle$ is zero. When c falls below c_{crit}, both the tip trajectory and the F_f curve are triple-valued functions of x_M; an example of the latter is labeled "soft" in Fig. 3. In this "soft" spring case, the tip snaps forward at the point of "instability," as in the "strong" spring case in the IO model above, giving the asymmetric F_f versus x_M curve shown by the curve with arrows. Here, the average friction force, given by the dashed line, is nonzero. The energy dissipated by the collapse of the elongated spring, calculated according to Eq. (1), is represented by the shaded area under a portion of the F_f versus x_M curve.

Figure 4 gives the average friction for a range of values of horizontal spring constant c and external force F_{ext}. Two results are apparent. First, the ability to measure a *zero friction* process depends on the value of c. Second, the friction coefficient $\mu = \langle F_f \rangle / F_{\text{ext}}$ for atomic contacts is not independent of load. Further discussion of friction versus load behavior for atomic sliding is given elsewhere.[31,32]

These simplified models of friction between atomic couples provide analytical criteria for transitions to zero friction, thus zero energy-dissipation conditions at $T = 0$ K. Zero friction requires "weak" interaction forces (low atomic-scaled corrugations) to achieve adiabatic motion and "hard" horizontal springs to measure the effect. An atomic "stick-slip" phenomena is predicted when these criteria are not met. The models are, in fact, consistent with atomic scale FFM measurements.[4]

B. MD simulations of monolayer films

MD simulations of friction behavior go beyond the simple analytical models. They use more realistic interaction potentials that exhibit anisotropy in two or three dimensions and they account for effects of temperature and sliding velocity. Moreover, video animations of the simulations allow us to visualize the trajectories of the atoms at and near the interface. MD thereby gives us our "first look" at what happens at the buried interface during sliding contacts. Early examples of MD studies of frictional contact between solid surfaces depicted wear and transfer of material in the sliding contact.[24,34] More recently, two studies of "wearless" friction have been reported; "wearless" friction means that no atoms are lost from or transferred to either member of the couple. In both studies, the solid surfaces were terminated with a monolayer of a simple hydrocarbon or hydrogen. This section presents these studies, which begin to address the role of surface films in friction processes.

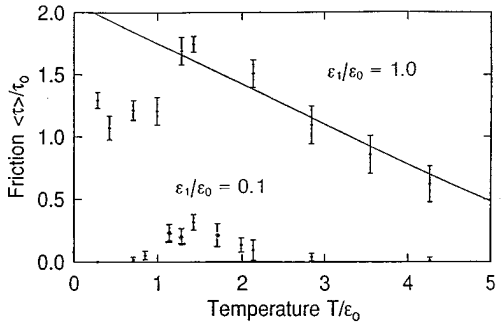

FIG. 5. Friction vs temperature data in normalized units for the case of strong ($\epsilon_1/\epsilon_0 = 1.0$) and weak ($\epsilon_1/\epsilon_0 = 0.1$) interfacial interactions at a sliding speed, $v = 20$ m/s. The solid line represents a fit to the data using a thermal activation model (Ref. 35).

1. Monolayers of alkane chains

McClelland and Glosli[30,35] have performed MD simulations of friction between two monolayers of alkane chains. The chains, six carbon atoms long, are initially ordered in a herringbone pattern. Chain bonds are allowed to bend and twist, but not stretch. Carbon and hydrogen atoms on each chain interact with atoms of other chains by a Lennard-Jones potential of interaction strength ϵ_0. The interaction strength at the interface ϵ_1 is adjustable in order to study its influence on friction behavior. The temperature of the layers is held constant by means of a heat bath; energy losses in the chains can thus be followed as heat losses in the layers. MD calculations are performed over a temperature range of $0 < T < 300$ K and sliding velocities up to $v_0 = 204$ m/s. The friction force is calculated as the shear stress τ averaged over several cycles of sliding.

Figure 5 shows two sets of friction versus temperature data for the case of strong ($\epsilon_1/\epsilon_0 = 1.0$) and weak ($\epsilon_1/\epsilon_0 = 0.1$) interactions at a sliding speed of $v = 20$ m/s. For both cases, the friction force exhibits different behaviors in the three (low, medium, and high) temperature regimes; in addition, for the case of weak interactions, the friction vanishes at low and high temperatures. In order to interpret the friction behaviors and energy dissipation processes, McClelland and

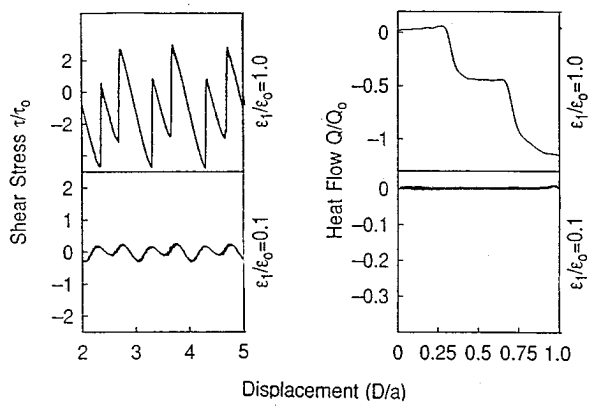

FIG. 6. Shear stress (left) and heat flow (right) vs sliding displacement for strong ($\epsilon_1/\epsilon_0=1.0$) and weak ($\epsilon_1/\epsilon_0=0.1$) interfacial interactions at $T=20$ K. The "zero" heat flow line, in lower right box, was added by present author (Ref. 35).

Glosli relied on video animations of the molecular dynamics and calculations of both shear stress and heat flow versus displacement curves.

At low temperatures, the trajectories of the alkane chains are very much like that of the atom-on-a-spring in the IO model discussed earlier. For strong interactions, the ends of the chains are strained until the local minimum in the potential disappears and the ends are released abruptly. The chains oscillate with a pivoted-hinge motion, retaining their herringbone pattern. At this temperature, chain oscillations cause the CH_x groups on the backbone to vibrate but do not induce torsional (twisting) motion of the chains themselves, i.e., vibration and twisting modes are decoupled at low temperatures.

Friction force versus distance curves exhibit atomic stick-slip, as seen in the upper left of Fig. 6. At slip, strain energy is released abruptly (25 ps), which caused the heat flow shown in the upper right of Fig. 6. Because the energy dissipation is associated with a plucking instability, the friction is expected to be independent of velocity; this was confirmed by MD calculations at several velocities for $T=20$ K. Plucking motion and energy dissipation occur until the interfacial interaction ratio falls below $\epsilon_1/\epsilon_0=0.4$. Below this value, the friction force versus distance curves vary smoothly and symmetrically about $F_f=0$ and there is no measurable heat flow (see lower left and right parts of Figs. 6, respectively). Like the weakly interacting atom in the IO model, the weakly coupled alkane chains exhibit harmonic motion as the two substrates slide past each other.

As the temperature increases, the friction in both interaction ranges increases, reaching maximum values around $T=80$ K. At this temperature, video animations depict very complex dissipation modes. The strain energy released by the bent chain now couples into three different modes: chain oscillations, CH_3 group vibrations and, for the first time, the torsional (twisting) modes. Torsional modes, which are "frozen" at lower temperatures, become excited at intermediate temperatures; this process is sometimes referred to as "rotational melting." With all three modes now anharmonically coupled, excitations damp out quickly as the energy is transferred to lattice vibrations in the substrate. Hence, the increase in friction at intermediate temperatures can be attributed to the excess energy associated with the unfrozen torsional modes.

As the temperature increases above the rotational melting temperature, a third mechanism comes into play: molecules vibrate so actively in all directions that an increasing percentage of the chains can hop and slide over the opposite surface without introducing strain. This reduces the net frictional force in both weak and strong interaction cases; in fact, in the weak interaction system, the friction force goes to zero at highest temperatures.

Glosli and McClelland then demonstrate that the friction behavior at high temperatures is consistent with classical behavior of polymeric films. MD calculations of strongly interacting couples showed increasing friction (sublinear) with sliding velocity (not shown here) and decreasing friction with temperature (Fig. 5). The latter curve was fitted to the Eyring thermal activation model that Briscoe and Evans[36] used to describe the shear behavior of thin polymeric films. The straight-line fit, drawn in Fig. 5, required only one adjustable parameter, the activation energy Q; it was determined to be $Q=70$ K. The shear strength (at $T=0$ K) derived from Q was $\tau=32$ MPa, about the same value obtained extrapolating to $T=0$ K Briscoe and Evans' experimental data for stearic acid (C18) and behenic acid (C22).

In summary, MD simulations of friction behavior between monolayers of alkane chains show that the simple harmonic versus plucking friction behavior applies to more complicated systems; in addition, the simulations enumerate the modes of dissipation that arise with increasing molecular complexity and increasing thermal activation.

2. H- and (H+C_xH_y)-terminated diamond (111) surfaces

Harrison, White, Colton, and Brenner[37–39] have simulated the friction behavior of H- and (H+C_xH_y)-terminated diamond (111) surfaces placed in sliding contact. The forces are derived from an empirical hydrocarbon potential capable of modeling chemical reactions in diamond and graphite lattices as well as small hydrocarbon molecules.[40] Two diamond (111) surfaces, each terminated in a (1×1) pattern, are placed in twin (mirror–image) contact; the distance of separation depends on the repulsive interaction potential and the load. Sliding is performed in two directions: the $[11\bar{2}]$ direction and the [110] direction. In the $[11\bar{2}]$ direction, opposing hydrogen atoms can make "head-on" contact at very high loads because their velocity vectors lie in a common plane perpendicular to the surface; this will be called the "aligned" direction. In the [110] direction, the hydrogen atoms can only pass adjacent to each other (across each others' diagonals) because their velocity vectors do not lie in a common perpendicular plane. The lattice temperature is set at 300 K, unless otherwise stated, and sliding velocities are 50 or 100 m/s. Normal loads are varied up to 0.8 nN/atom, corresponding to mean pressures up to 20 GPa, and friction coefficients are averaged over a unit cell.

Their first study examines two H-terminated diamond (111) surfaces.[37] Along the $[11\bar{2}]$ direction, the friction coef-

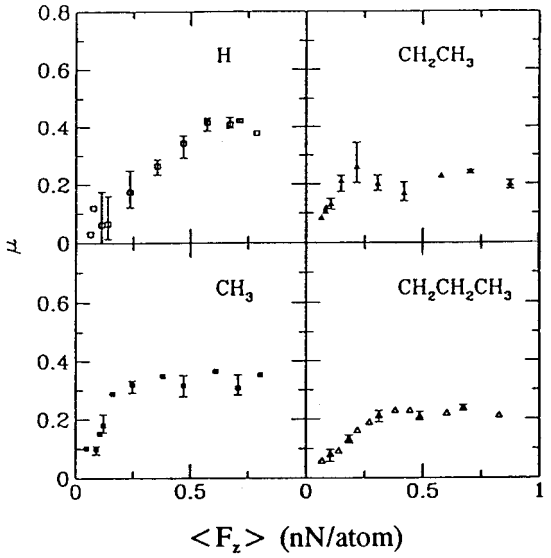

FIG. 7. Average friction coefficient as a function of normal load for (H $+2X$)-terminated surfaces sliding in the [112] direction at $v=1$ Å/ps and at $T=300$ K. Curves are for X=hydrogen, methyl, ethyl, and *n*-propyl-terminations, respectively. From Ref. 39.

ficient begins near zero for lowest loads, increases nearly linearly with load up to 0.6 nN/atom, then levels out at $\mu=0.4$ (see Fig. 7).

Video animation sequences of sliding along the "aligned" [112] direction show different interaction mechanisms at low and high loads. At lowest loads, opposing hydrogen atoms first repel each other backwards. Then as strain develops, they pivot sideways and revolve past each other at closest approach, finally pushing each other forward. With these trajectories, the net frictional force, averaged over a unit cell, nearly cancels and almost no energy is dissipated. At higher loads, atomic-level stick-slip occurs: instead of gently revolving by each other, opposing hydrogen atoms momentarily become "stuck" in a (mutually) repulsive potential well, then suddenly "slip" and revolve around one another. The pivoting-then-revolving motion, assisted by thermal motion, excites both vibrational and bending modes in the C–H bonds. These excitations are passed on to the lattice as vibrations (phonons) then heat. In this way, potential (strain) energy developed at high loads is transformed into kinetic energy (mechanical excitations), leading to nonzero values of the friction coefficient.

Friction coefficient versus load data for sliding along the [110] direction (not shown here) are about an order-of-magnitude lower than along the [112] direction. Animations show that hydrogen atoms, instead of meeting along aligned directions, "zigzag" through channels of potential minima that run between adjacent rows of hydrogen atoms on the opposing surfaces. Since the opposing hydrogen atoms do not encounter each other directly, strain levels are lower and thus the frictional forces are lower. Hence, different sliding directions on identical surfaces lead to anisotropy in both atomic trajectories and friction coefficients. Perhaps these trajectories can account for the well-know frictional anisotropy of single crystals.[41,42]

The friction coefficient of the H-terminated surface shows a temperature dependence that is qualitatively similar to that found with alkane chains. At a fixed pressure of 3 GPa, the friction coefficient at $T=0$ K is high ($\mu=0.4$), but drops as the temperature rises: to $\mu=0.25$ at 70 K, then to $\mu=0.15$ at 300 K. The friction coefficient is larger at low temperatures because opposing hydrogen atoms cannot rotate out of the way of aligned-trajectory repulsive wells without the help of thermal motion.

Harrison *et al.*[38] have also examined the friction behavior of the same sliding configuration of H-terminated diamond but with two methyl groups substituted for two hydrogen atoms on one surface. Along the [112] direction, the friction coefficient versus load data rise quicker than on the fully H-terminated surface, but reach lower steady-state values ($\mu=0.35$ versus $\mu=0.4$) (see Fig. 7). These differences can be attributed to the large volume occupied by a methyl group. Instead of easily "revolving" around the hydrogen atoms during low-load, aligned-trajectory collisions, the methyl group gets stuck, then "slips" with a ratcheting motion. The ratcheting motion, analogous to the motion of a "turnstile," rotates the methyl group alternately clockwise then counterclockwise 120° around the C–C bond. Turnstile motion, accompanied by C–H bond excitations, is responsible for higher friction at low loads. At high loads, the size of the methyl groups keeps the two surfaces further apart than comparably loaded H-terminated pairs. Harrison[43] speculates that the "flattening" out of the friction coefficient versus load data may be due either to screening of the interaction potential or to constraining the excitation modes.

Sliding the methyl-substituted surface along the $[\bar{1}10]$ direction (not shown) produces the same, strong load-dependent friction coefficients found in the [112] direction (see Fig. 7). Remarkably, the substitution of two CH_3 molecules for two hydrogen atoms produces an order of magnitude greater friction coefficient. Why? Unlike the terminal hydrogen atoms, which can "zigzag" freely through the adjacent hydrogen atom channels, the larger methyl groups exhibit "turnstile" rotations like those found in [112] sliding. The rotations are accompanied by "zigzag" motion, which becomes more pronounced as the load increases. The increased energy expended by the larger molecules in this turnstile and zigzag trajectory is responsible for the increase in friction coefficient with load.

In their latest study, Harrison *et al.*[39] have substituted two ethyl and two *n*-propyl groups for two hydrogen atoms; friction coefficient versus load data are seen in the two right panels of Fig. 7. The larger, more flexible hydrocarbon groups reduce friction at high loads by a factor of 1.5 to 2 compared with the fully H-terminated diamond slider. Center-of-mass trajectories of the CH_3 portion of the ethyl groups, plotted on potential energy contour maps of a H-terminated diamond (111) surface, give insight into how the motion of an ethyl molecule affects the friction coefficient. At low loads (not shown here), the ethyl molecule bends over, lies down, and is dragged almost straight across the repulsive potentials, like the trajectory a chain would have if one end were tied to the upper surface. At high loads, however, the ethyl molecule uses its flexibility and length to

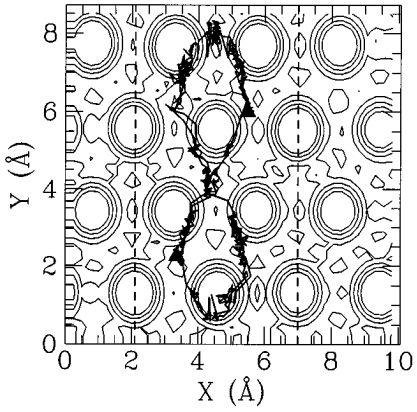

FIG. 8. Center-of-mass trajectories of the CH_3 tail of an ethyl group (dark solid line) plotted on a potential energy contour map of a H-terminated, diamond (111) surface. The two solid triangles indicate the starting points for two CH_3 tails. Sliding is along the *Y* direction. The two dashed lines represent the trajectories of the attachment point out the ethyl groups during sliding. Average normal force is 0.42 nN/atom. See Ref. 39 for details.

''snake'' (detour) around high potential energy barriers. This trajectory, depicted by solid lines in Fig. 8, expends less energy and produces a lower friction coefficient than the pivot-rotation or turnstile modes found with smaller molecules.

In summary, Harrison *et al.* have identified several mechanisms which may account specifically for the friction behavior and energy dissipation of hydrogen- and hydrocarbon-terminated diamond surfaces, and, more generally, for boundary film lubrication. They have shown that, at 300 K, hydrogen- and hydrocarbon-terminations follow different trajectories when sliding along ''hard'' (aligned-trajectory) and ''soft'' (channels) directions of H-terminated diamond, and thereby explain the strong frictional anisotropy of H-terminated diamond pairs along selected low-friction channels. They have cataloged numerous excitation modes (rotations, turnstiles, ...) by which frictional energy is dissipated. In addition, they have shown that, at high contact stresses, larger hydrocarbon groups reduce friction even further because of size and steric effects.

III. EXPERIMENTAL APPROACHES

A. Friction and adhesion hysteresis

Israelachvili and co-workers[44] have recently discovered a new relationship between adhesion and friction, based on experimental studies of surfactant monolayers. Experiments are performed with a SFA, in which both adhesion and friction are measured. Adhesion behavior is examined in contact radius versus load curves during loading–unloading cycles and in pull-off force measurements; friction behavior, in unidirectional and reciprocating sliding. The surfactant monolayers studied exhibit one of three phases: solidlike, amorphous, or liquidlike. The amorphous state is a phase in between the solidlike and liquidlike state. Moreover, the phases of each of the layers could be changed by varying the atmosphere, temperature, velocity or related parameters.

The main conclusion of the study is that the friction force does not correlate with the adhesion force (or adhesion en-

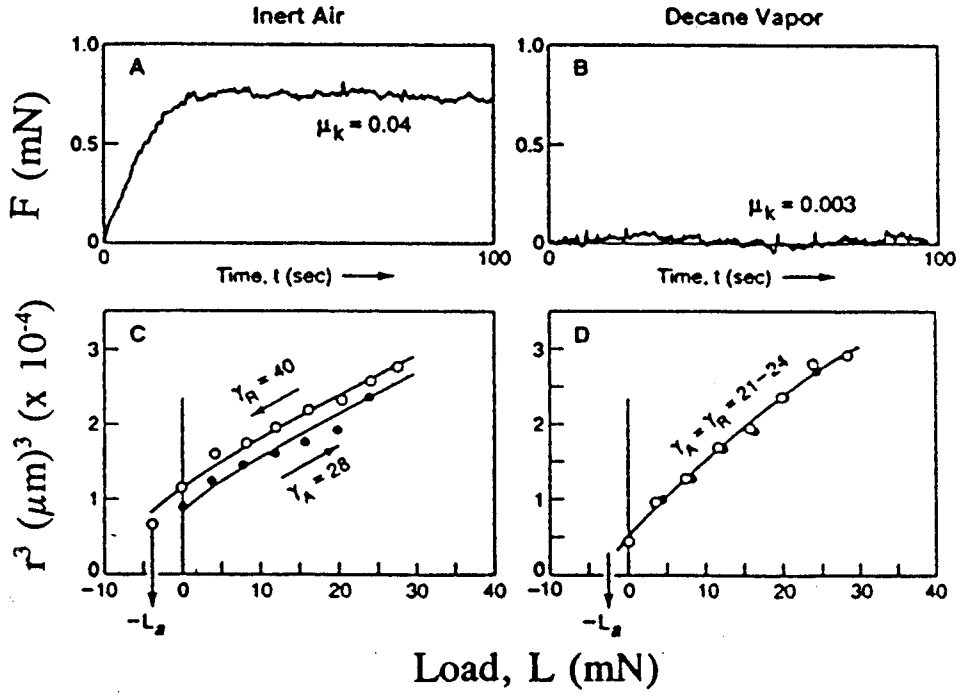

FIG. 9. (A) and (B) Friction traces of two CaABS monolayers at 25 °C exposed to inert air and to air saturated with decane vapor. (C) and (D) Adhesion energies on loading, unloading and pull-off measured under the same conditions as the upper friction traces (Ref. 44).

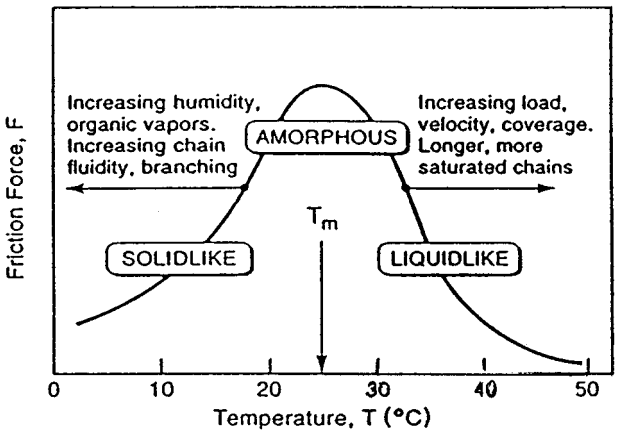

FIG. 10. A schematic "friction phase diagram" representing the trends observed in the friction forces of five different surfactant monolayer types studied. The curve also correlates with adhesion hysteresis of the monolayers but not with the adhesion *per se* (Ref. 44).

ergy γ), but rather with *hysteresis* in the adhesion force. As an example, Fig. 9 shows friction and adhesion measurements for loading and unloading two calcium alkylbenzenesulfonate (CaABS) monolayers at 25 °C. The curves to the left (A and C) represent behavior of a liquidlike monolayer: quite a low friction coefficient and some hysteresis in the adhesion during the loading–unloading cycle. The curves to the right (B and D) show that after exposing the surfaces to decane vapor, the already low friction coefficient decreases even more and the adhesion hysteresis disappears. Previous studies[45,46] had shown that when hydrocarbon vapors condensed onto CaABS, the molecules penetrated the outer chain regions and fluidized the surface. Thus, it was hypothesized that if the monolayer were made more liquidlike, the friction and adhesion hysteresis would be reduced.

Many other correlations between friction and adhesion hysteresis and the phase of surfactant monolayers have been observed. Both friction and adhesion hysteresis increase when solidlike monolayers or liquidlike monolayers are made amorphous. Conversely, when amorphous monolayers are made more fluidlike or solidlike, both the friction and adhesion hysteresis decrease.

Observed trends in friction and adhesion hysteresis behavior are summarized in the schematic "friction phase diagram curve" shown in Fig. 10. Maximum values of friction and adhesion hysteresis (*but not adhesion values*) are found around a "chain-melting" temperature T_m; this is the temperature at which the monolayer is inbetween the solidlike and liquidlike state, i.e., the amorphous state. Lower values of friction and adhesion hysteresis are found at temperatures above or below T_m. It is seen that the amorphous state represents the highest friction and highest adhesion hysteresis. Factors that can change the phase state of monolayers, such as vapors, speed, etc., can effectively shift the curve in directions indicated by the arrows in Fig. 10.

Israelachvili *et al.*[44] give a physical basis for this behavior. Adhesion hysteresis is the "irreversible" part of the adhesion energy, and is related to the energy dissipated during the loading and unloading process. A likely molecular origin of adhesion hysteresis is the extent of interpenetration and subsequent ease of disentanglement of the molecules across an interface. If there is little interpenetration, as with solidlike layers, the friction is smooth and no additional energy is expended separating surfaces. If there is significant interpenetration, as with liquidlike layers, but also ease of disentanglement on separation, the friction is again low and little extra energy is expended separating surfaces. A thermodynamic description of the liquidlike case would conclude that the time to separate the chains is slower than the relaxation time of the molecules and, therefore, that separation approximates a reversible process. In both the above cases, the systems are physically in similar states going into and coming out of contact. By contrast, with amorphous layers, there is significant chain interpenetration but separation occurs faster than the molecular relaxation time. Thus, amorphous layers will be in different states going into and coming out of contact, and consequently, more energy will be expended to separate them than would be needed for the two other phases.

This new mechanism of friction in boundary lubrication can operate over a wide time scale, the time it takes a particular molecule to adapt its trajectory to the lowest possible interaction potential, relative to the time-dependence of the potential. In the case of the MD studies of *n*-propyl-terminated diamond,[39] the low friction was achieved at high loads because the molecules could "follow" the lowest energy contours in picoseconds. The same was true for the liquidlike monolayers, whose chains could follow the minimum force trajectories in milliseconds.[44] However, on the same time scale, amorphous chains could not follow minimum force trajectories, and energy differences were seen in both adhesion hysteresis and friction.

B. Friction and slip of monolayer films

Krim *et al.*[15–17] are studying the frictional forces for solidlike and liquidlike films adsorbed on conducting (metal) and insulating (oxidized metal) substrates. Their approach is quite novel. Films of gases such, as Kr and Ar or C_2H_4 and C_2H_6, are condensed onto surfaces to thicknesses up to several monolayers. The thickness of the film is determined in a straight-forward manner with a QCM. In addition, the QCM monitors subangstrom shifts in the vibrational amplitude caused by gas adsorption. These shifts are due to frictional shear forces between the condensing film and the oscillating surface. Krim *et al.*[15] have shown that the "slip time" τ of a monolayer film can be determined with subnanosecond accuracy from these shifts. Note that the time and length scales, nanoseconds and angstroms, makes these experiments unique in the field of tribology. Since slip is fundamentally an energy-dissipative process, the technique allows energy dissipation to be measured and the mechanisms of energy dissipation to be studied.

Experiments with rare gas atoms have shown that (1) the slip times for monolayers physisorbed on smooth gold surfaces are on the order of nanoseconds and (2) solidlike films exhibit longer slip times than liquidlike films. These results

are consistent with a frictional force proportional to the sliding velocity, indicating a viscous friction mechanism.

Three models have been proposed to account for energy dissipation of the sliding monolayers. The first two postulate that phonons carry away the energy. Sokoloff, using an analytical model of friction,[47,48] suggests that defects between the incommensurate monolayer–solid interface can account for the slip times. Robbins *et al.*[49] have used molecular dynamic simulations to determine the viscous coupling between a driven substrate and an adsorbed monolayer film. Requiring no arbitrary parameters, the model gives excellent agreement with many of the experimental observations: it gives the correct magnitude of slip time τ; a friction force proportional to τ for physisorbed films; and less slip in liquid films than in solid films. They have also shown that their results agree with a simple analytic model, closely related to that of Sokoloff. The slip time is directly related to equilibrium properties of the film: it is proportional to the lifetime of longitudinal phonons and inversely proportional to the square of the density oscillations induced by the substrate.

A third model, presented by Persson *et al.*,[50] postulates energy dissipation by electron–hole scattering. It assumes that electrons in the metal substrate experience a drag force equal in magnitude to the force required to slide the adsorbed film. This force is estimated from measurements of the change in resistivity of metal films as a function of gas coverage. Calculated slip times are in good agreement with experimental values for adsorbed rare gases and hydrocarbon molecules. The model also predicts different slip times for C_2H_4 and C_2H_6 adsorbate films, but only if electronic contributions are present, e.g., with metals but not insulators. Krim's group[51] has recently tested this prediction by measuring slip times for C_2H_4 and C_2H_6 on silver and on oxygen-coated silver. They find *different* slip times on Ag, but *the same* slip time on oxygen-coated silver, consistent with the predictions. Thus, based on these rather unique studies of friction, it appears that both phonon and electron mechanisms contribute to energy dissipation.

IV. SUMMARY AND DISCUSSION

From studies just reviewed and others in the literature, our understanding of interfacial friction processes and energy dissipation mechanisms can be summarized as follows. Low friction, including zero friction, can be achieved at low loads, with weak interface interactions and with ''small'' atoms at the interface. The mechanical principle that explains this behavior follows from the simple, one-dimensional, IO model: the strain energy transmitted by interfacial atoms during the first half of the cycle is returned to them during the second half-cycle. This behavior is also observed in the more realistic, three-dimensional MD simulations. The third dimension itself contributes an additional friction reduction channel; it provides the interfacial atoms an extra degree of freedom—to move out of their common plane—to escape ''stick'' events along aligned directions. For example, H-terminated atoms can rotate around each other or ''zigzag'' along potential minima channels; these trajectories are not available to atoms described in two-dimensional models. In principle, many ''low friction trajectories'' can be found along selected directions in real crystals having anisotropic interaction potentials (corrugations); these possibilities are treated more quantitatively by Hirano and Shinjo.[52] In practice, however, too soft a spring in the measuring device can lead to friction force instabilities, resulting in measured friction forces that are higher than expected.

Friction is increased by many factors. Strong interfacial interactions (corrugations), according to the simple IO model, give a finite static friction force, then stick-slip motion between atoms. Three-dimensional potentials also show atomic-scale stick-slip processes, but produce modes, e.g., turnstile motion, that are more complex than the equivalent two-dimensional plucking mode. Atomic-scale stick-slip processes have been seen in FFM measurements, but at present the modes responsible have not been identified because of the relatively slow response time of friction devices.[53] Anharmonic coupling of excited modes establishes multiple pathways for energy dissipation, thereby increasing friction coefficients. An example is the MD simulation of alkanes at intermediate temperatures, where torsional modes become allowed, providing a new pathway for energy dissipation. Other excitation modes that enhance friction and dissipate energy are density oscillations, defects at interfaces and electron–hole coupling in metals. Commensurate lattices have been shown to increase friction forces by many orders of magnitude.[47] Friction force is expected to increase with increasing external force (load). However, as Zhong and Tománek[33] have shown, surface interactions can be perturbed over a selected load range, thereby lowering the friction coefficient as the load increases.

Temperature can influence friction behavior in several ways. Thermal activation of an energy-dissipating mode, like rotational melting, increases friction. In contrast, thermal activation can lower potential barriers and increase tunneling, thereby reducing friction. At high temperatures, thermal effects can dominate friction processes, giving liquidlike (viscous) friction instead of solid friction (finite static friction at all velocities). The MD simulation of alkane chain friction showed this transition from solid to viscous behavior with increasing temperature.

The size and shape of molecules can also influence friction behavior. Small atoms or molecules may follow low-friction trajectories whereas larger atoms or molecules may not ''fit'' into the same channels, resulting in higher friction. The H- versus CH_3-terminated diamond along the $[1\bar{1}0]$ direction is such an example. By contrast, larger molecules can reduce friction more effectively than smaller molecules at higher loads if they have sufficient flexibility to spread across the surface; an example is the high load behavior of the hydrocarbon-terminated diamond surfaces. This steric accommodation, however, can increase friction if the molecule cannot follow the minimum-energy trajectory as fast as the surfaces move apart. Chain entanglement between amorphous films observed in SFA studies is an example of steric effects causing increased energy dissipation.

A new concept of friction behavior has been demonstrated by Israelachvili *et al.* that energy dissipation is maximum

when the time (and length) scales of contact (externally controlled) match the intrinsic time and length scales of molecular interactions. This concept is consistent with thermodynamic considerations of two bodies coming into contact. As mentioned in the introduction, the degree to which the contact process approximates a reversible, quasistatic process depends on the rate at which each step is taken compared to the relaxation time of the system. Put in terms of the driven oscillator analog, deviations from equilibrium and energy dissipation are maximum when time and length scales of the system and driver are matched. However, classical thermodynamics is not really suitable for the treatment of contacting surfaces let alone sliding surfaces. Even in the mildest contact circumstances, in which the two bodies retain their identity after separating, equilibrium was never achieved; at best, the two bodies reached metastable equilibrium. A more precise description of the thermodynamics of contacting surfaces is needed.

Finally, these studies can give us some new insights into the role of surface films in friction processes. Generalizing the studies of Harrison *et al.*, we see that films in which ''small'' atoms chemisorb one-to-one with the substrate lattice might provide the screening needed to prevent interface ''welding'' and give low-friction trajectories along weak corrugation channels. Films made of larger molecules, with lower compressibility, might reduce friction at high loads by providing atomic screening as well as steric accommodation.

V. RECOMMENDATIONS

This review was meant to introduce tribologists to some of the more recent investigations of energy dissipation processes in interfacial friction. Many recommendations for future research in atomic-scale tribology can be made based on these preliminary investigations. For example, the remarks in the previous paragraph suggest two approaches for modeling boundary lubricant films: (1) gas or solute/additive interactions with surfaces can be modeled with small, single-atom terminations and (2) ''run-in'' boundary films can be modeled by more complex molecular attachments.

Many of the ideas discussed in this paper were presented at a two week long NATO ASI meeting held in Braunlage, Germany in August 1991. Considerable time was spent discussing ''future issues'' and suggested approaches for research in this field; these have been published in the Epilogue to the conference proceedings.[54] Here I summarize only a few of these items.

(1) How can atomistic modeling continue to make an impact on understanding friction? on understanding lubrication?
(2) Can algorithms (e.g., hybrid methods) be developed to simulate friction processes at time and length scales longer than can be treated in molecular dynamics calculations alone, e.g., that extend computational simulations from the nm/fs scale to the μm/μs scale.
(3) Can lubricants be tailored to take advantage of the dynamic properties of certain fluids, e.g., the ''chemical hysteresis'' of monolayer films discussed by Israelachvili *et al.*
(4) In practical machines, sliding is sustained on surface films—whether organic lubricants, oxides, or other solid films. Can molecular simulations help us to understand the chemistry of film formation, the mechanical properties of these films and how the films break down?

One of the newest issues that tribology must deal with is the concept of matching time and lengths scales in friction studies. As we saw above, energy dissipation hence friction is intimately linked to time and length scales. Moreover, the atomic/molecular modes of interfacial interactions operate at time and length scales far shorter than traditional tribology measurements. In the section of the Epilogue[54] entitled *New ways of probing friction processes*, we asked ''How can we use the power of microscopic modeling to gain new insights into macroscopic friction processes and, ultimately, to solve technological problems?'' Goddard[55] suggests that this can be done by progressing along the ''chain-linked'' ladder, illustrated in Fig. 11, from quantum-level studies to engineering design. His ''hierarchy of modeling tribological behavior'' unites atomistic models, which operate in very short length-time scales, with engineering models, which describe tribological behavior in length-time scales observable by more traditional measuring equipment. This approach ''...allows consideration of larger systems with longer time scales, albeit with a loss of detailed atomic-level information. At each level, the precise parameters (including chemistry and thermochemistry) of the deeper level get lumped into those of the next. The overlap between each level is used to establish these connections. This hierarchy allows motion up and down as new experiments and theory lead to new understanding of the higher levels, and new problems demand new information from the lower levels.''

But where are the experimental approaches for investigating the ''lower (short scale) levels?'' As illustrated in Fig. 11, most ''friction machines,'' including the proximal probe devices, are operated at long time scales. An abbreviated search of recent literature produced only three ''tribology'' tests and a fourth proximal probe method that come close to investigating friction behavior at short time and length scales. Labeled (1)–(4) in the Fig. 11, they are described here briefly.

(1) Bair *et al.*[56] have used fast IR detectors to measure flash temperatures during high speed frictional contacts of asperities of length 10 μm and greater, with time resolution of about 20 μs.
(2) Spikes *et al.* have developed *real time* optical techniques for investigating the physical behavior of EHL films down to 5 nm thick[57] and chemical processes occurring in contacts 10 μm wide by 80 nm thick.[58]
(3) Krim *et al.*[15,16] have used the quartz crystal microbalance experiments (described earlier) for probing atomic vibrations amplitudes between 0.1 and 10 nm and time scales from 10^{-12} to 10^{-8} s.
(4) Hamers and Markert[59] have shown that STM images are sensitive to the recombination of photoexcited carriers whose lifetimes are in the picosecond range.

Clearly, innovative experimental approaches for measuring friction processes at short and intermediate time-length

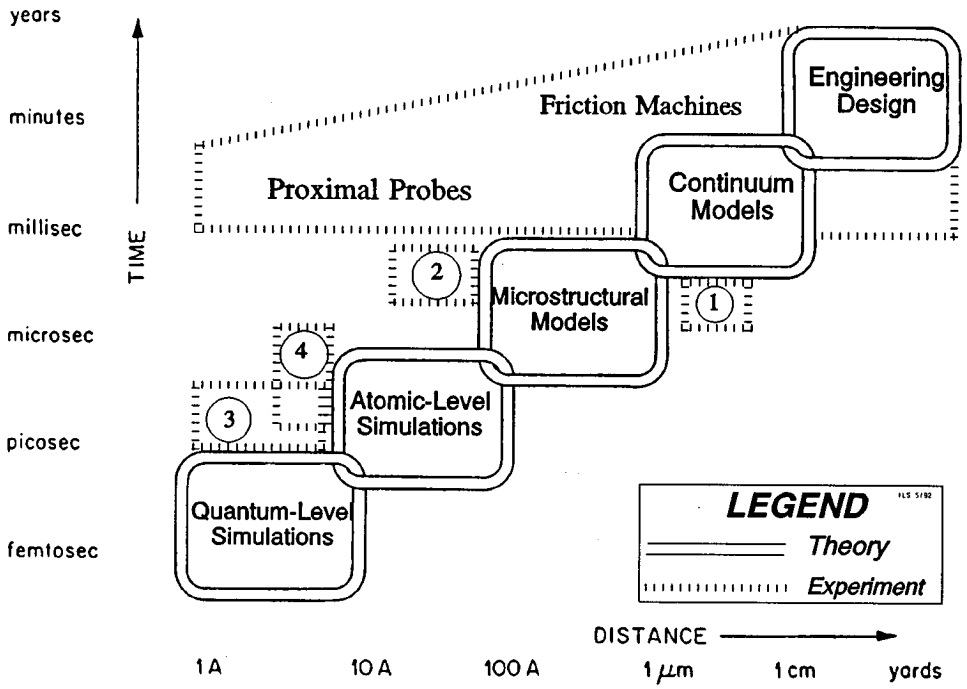

FIG. 11. Time and length scales of present-day models and experiments in Tribology. From Ref. 54.

scales are needed to assist the modelers who are already there. Tribologists should seek out physicists and chemists working in these time-space domains and form collaborations to carry out tribology-oriented experiments. As I have tried to emphasize in this article, much of the progress in the field comes when experiments and theories can overlap on the same time-length scales.

Finally, there is another time scale to consider, and that is "the question of time to translating this (fundamental) knowledge into engineering practice." Professor Dowson (Leeds University, UK) told us how this can be accomplished in the final part of the Epilogue.[60]

"We have heard quite a lot about the subject of friction from the atomic scale up to the macroscopic scale....

There are other aspects of scale I think we should reflect on. One is the question of time in terms of translating this knowledge into engineering practice... The time scales are generally *enormous*. ...I think you should take note that it is going to be about A DECADE IF NOT A GENERATION before that impact will be seen fully in engineering. This makes it all the more important for ... physicists, chemists and engineers (to meet), so that the engineers can absorb by osmosis the concepts that you are revealing.... It is important that these ideas feed into our consciousness so that we apply them sensibly in future developments.

...I hope equally that scientists will not be too frustrated by the fact we take 10 to 20 years to incorporate their bright new ideas in designing better skis or whatever it might be. Let us perpetuate this interaction between groups of people who all have one objective and that is to understand the laws of physics in order to apply them as effectively as we possibly can for the good of society through the manufacture of reliable, efficient and sensible products."

ACKNOWLEDGMENTS

The author is most grateful to the following colleagues for providing reprints and preprints and their willingness to engage in discussions of their results: J-M. Georges, J. A. Harrison, J. N. Israelachvili, J. Krim, G. M. McClelland, H. M. Pollock, M. O. Robbins, J. B. Sokoloff, and D. Tománek. He is also grateful to the Laboratoire de Technologie des Surfaces, Ecole Centrale de Lyon, where this paper was conceived, and to ONR/NRL for financial support.

Presented at the Leeds-Lyon Symposium on Dissipative Process in Tribology, Villeur-banne, France, 7 September 1993.

[1] *Fundamentals of Friction*, edited by I. L. Singer and H. M. Pollock (Kluwer, Dordrecht, 1992).
[2] G. Binnig, H. Rohrer, Ch. Gerber, and E. Weibel, Phys. Rev. Lett. **49**, 57 (1982); Phys. Rev. Lett. **50**, 120 (1983).
[3] G. Binnig, C. F. Quate, and Ch. Gerber, Phys. Rev. Lett. **56**, 930 (1986).
[4] C. M. Mate, G. M. McClelland, R. Erlandsson, and S. Chiang, Phys. Rev. Lett. **59**, 1942 (1987).
[5] G. Meyer and N. M. Amer, Appl. Phys. Lett. **56**, 2100 (1990).
[6] E. Meyer, R. Overney, L. Howald, D. Brodbeck, R. Lüthi, and H.-J. Güntherodt, in Ref. 1, p. 427.
[7] D. Tabor and R. H. S. Winterton, Proc. R. Soc. London, Ser. A **312**, 435 (1969); J. N. Israelachvili and D. Tabor, Proc. R. Soc. London, Ser. A **331**, 19 (1972).
[8] J. N. Israelachvili, P. M. McGuiggan, and A. M. Homola, Science **240**, 189 (1988); A. M. Homola, J. N. Israelachvili, P. M. McGuiggan, and M. L. Gee, Wear **136**, 65 (1990).
[9] J. N. Israelachvili, in Ref. 1, p. 351.
[10] A. Tonck, J. M. Georges, and J. L. Loubet, J. Colloid Interface Sci. **126**, 150 (1988).

[11]J-M. Georges, D. Mazuyer, A. Tonck, and J. L. Loubet, J. Phys. Cond. Mat. **2**, 399 (1990).
[12]J-M. Georges, D. Mazuyer, J-L. Loubet, and A. Tonck, in Ref. 1, p. 263.
[13]J. Van Alsten and S. Granick, Phys. Rev. Lett. **61**, 2570 (1988); S. Granick, Science **253**, 1374 (1991).
[14]S. Granick, in Ref. 1, p. 387.
[15]J. Krim and A. Widom, Phys. Rev. B **38**, 12184 (1988).
[16]J. Krim, D. H. Solina, and R. Chiarello, Phys. Rev. Lett. **66**, 181 (1991).
[17]J. Krim and R. Chiarello, J. Vac. Sci. Technol. A **9**, 2566 (1991).
[18]E. Rabinowicz, *Friction and Wear of Materials* (Wiley, New York, 1965), pp. 94–107.
[19]I. V. Kragelskii, *Friction and Wear* (Butterworths, Washington, 1965), pp. 208–218.
[20]J. B. Pethica and A. Sutton, J. Vac. Sci. Technol. A **6**, 2490 (1988).
[21]J. R. Smith, G. Bozzolo, A. Banerjea, and J. Ferrante, Phys. Rev. Lett. **63**, 305 (1989).
[22]J. Ferrante and G. Bozzolo, in Ref. 1, p. 437.
[23]U. Landman, W. D. Luedtke, and E. M. Ringer, Wear **153**, 3 (1992).
[24]U. Landman, W. D. Luedtke, and E. M. Ringer, in Ref. 1, p. 463.
[25]J. Leslie, *An Experimental Inquiry into the Nature and Propagation of Heat* (Bell and Bradfute, Edinburgh, 1804).
[26]D. Dowson, *History of Tribology* (Longman, London, 1979).
[27]K. L. Johnson, in Dissipative Process in Tribology, Proceedings of the 20th Leeds-Lyon Symposium on Tribology, Villeurbanne, France, 7–10 September 1993, edited by D. Dowson, C. M. Taylor, T. H. C. Childs, M. Godpet, and G. Dalmaz (to be published).
[28]H. B. Callen, *Thermodynamics* (Wiley, New York, 1960), p. 63.
[29]G. M. McClelland, in *Adhesion and Friction*, edited by M. Grunze and H. J. Kreuzer (Springer, Berlin, 1990), p. 1.
[30]G. M. McClelland and J. N. Glosli, in Ref. 1, p. 405.
[31]D. Tománek, W. Zhong, and H. Thomas, Europhys. Lett. **15**, 887 (1991).
[32]D. Tománek, in *Scanning Probe Microscopy*, edited by H.-J. Güntherodt and R. Wiesendanger (Springer, Berlin, 1993), Chap. 11.
[33]W. Zhong and D. Tománek, Phys. Rev. B **64**, 3054 (1990).
[34]J. Belak and I. F. Stowers, in Ref. 1, p. 511.
[35]J. N. Glosli and G. M. McClelland, Phys. Rev. Lett. **70**, 1960 (1993).
[36]B. J. Briscoe and D. C. Evans, Proc. R. Soc. London, Ser. A **380**, 389 (1982).
[37]J. A. Harrison, C. T. White, R. J. Colton, and D. W. Brenner, Phys. Rev. B **46**, 9700 (1992).
[38]J. A. Harrison, R. J. Colton, C. T. White, and D. W. Brenner, Wear **168**, 127 (1993).
[39]J. A. Harrison, C. T. White, R. J. Colton, and D. W. Brenner, J. Phys. Chem. **97**, 6573 (1993).
[40]J. A. Harrison, C. T. White, R. J. Colton, and D. W. Brenner, Surf. Sci. **271**, 57 (1992).
[41]D. H. Buckley, *Surface Effects in Adhesion, Friction, Wear, and Lubrication* (Elsevier, New York, 1981), pp. 357–373.
[42]M. Hirano, K. Shinjo, R. Kaneko, and Y. Murata, Phys. Rev. Lett. **67**, 2642 (1991).
[43]J. A. Harrison (private communication, 1993).
[44]H. Yoshizawa, Y-L Chen, and J. Israelachvili, J. Phys. Chem. **97**, 4128 (1993).
[45]Y. L. Chen, C. A. Helm, and J. N. Israelachvili, J. Phys. Chem. **95**, 10736 (1991).
[46]Y. L. Chen and J. N. Israelachvili, J. Phys. Chem. **96**, 7752 (1992).
[47]J. B. Sokoloff, Phys. Rev. B **42**, 760 (1990); Wear **167**, 59 (1993).
[48]J. B. Sokoloff, Thin Solid Films **206**, 208 (1991); J. Appl. Phys. **72**, 1262 (1992).
[49]M. Cieplak, E. D. Smith, and M. O. Robbins, Science (in press).
[50]B. N. J. Persson, D. Schumacher, and A. Otto, Chem. Phys. Lett. **78**, 204 (1991); Phys. Rev. B **44**, 3277 (1991).
[51]C. H. Mack, C. Daly, and J. Krim, Thin Solid Films (in press).
[52]M. Hirano and K. Shinjo, Phys. Rev. B **41**, 11 837 (1990).
[53]I. L. Singer and H. M. Pollock, in Ref. 1, p. 582.
[54]I. L. Singer and H. M. Pollock, in Ref. 1, p. 569.
[55]*Tribology of Ceramics*, National Materials Advisory Board Report 435 (National Academy, Washington, DC, 1988), p. 88.
[56]S. Bair, I. Green, and B. Bhushan, J. Tribology **113**, 547 (1991).
[57]G. J. Johnston, R. Wayte, and H. A. Spikes, Tribology Trans. **34**, 187 (1991).
[58]P. M. Cann and H. A. Spikes, Tribology Trans. **34**, 248 (1991).
[59]R. J. Hamers and K. Markert, Phys. Rev. Lett. **64**, 1051 (1990).
[60]I. L. Singer and H. M. Pollock, in Ref. 1, p. 586.